Record-High In-Device Electro-Optic Coefficient of 359 pm/V in a Silicon-Organic Hybrid (SOH) Modulator

C. Kieninger[(1,2)]*, Y. Kutuvantavida[(1,2)], H. Zwickel[(1)], S. Wolf[(1)], M. Lauermann[(3)], D. L. Elder[(4)], L. R. Dalton[(4)] W. Freude[(1)], S. Randel[(1)] and C. Koos[(1,2)]**

(1) Karlsruhe Institute of Technology (KIT), Institute of Photonics and Quantum Electronics (IPQ), Karlsruhe, Germany
(2) Karlsruhe Institute of Technology (KIT), Institute of Microstructure Technology (IMT), Karlsruhe, Germany
(3) Now with: Infinera Corporation, Sunnyvale, CA, USA
(4) University of Washington, Department of Chemistry, Seattle, USA
*Author e-mail address: *clemens.kieninger@kit.edu, **christian.koos@kit.edu*

Abstract: We demonstrate a record-high electro-optic coefficient of r_{33} = 359 pm/V in a silicon-organic hybrid (SOH) modulator using the electro-optic chromophore JRD1. The π-voltage-length product amounts to $U_\pi L$ = 320 Vµm, enabling error-free 25 Gbit/s signaling at drive voltages of 180 mV_{pp}.

OCIS codes: (160.2100) Electro-optical materials; (230.2090) Electro-optical devices; (250.5300) Photonic integrated circuits

1. Introduction

The silicon-organic hybrid (SOH) integration concept combines silicon photonic waveguide structures with organic electro-optic (EO) cladding materials, thereby leveraging both the benefits of large-scale standardized CMOS processing and the wealth of optical properties obtained by theory-guided molecular design of organic chromophores [1]. Over the last years, SOH EO modulators have been demonstrated to feature record performance parameters with respect to efficiency [2,3], bandwidth [4] and achievable data rates [5,6], also at elevated temperatures of 80 °C [7]. This progress was enabled by continuous improvements of the underlying EO materials, in particular with respect to the achievable in-device EO coefficient r_{33}. The highest value demonstrated so far amounts to r_{33} = 230 pm/V, achieved for the binary-chromophore organic glass system PSLD41/YLD124 [3].

Here we demonstrate that even higher EO coefficients can be achieved by theory-guided optimization of both molecular hyperpolarizability and poling efficiency. We use the EO chromophore JRD1 [8], which relies on the same chromophore core as the previously used YLD124, complemented by functional side groups that allow efficient alignment even at high number densities without a polymer host. When deposited onto a slot-waveguide SOH modulator, this material shows an in-device EO coefficient of r_{33} = 359 pm/V. This is the highest in-device EO coefficient ever demonstrated for any material system. The EO modulator features a π-voltage-length product of $U_\pi L$ = 320 Vµm – the smallest value ever demonstrated for a non-resonant device based on low-loss dielectric waveguides. We demonstrate the viability of the device by generating error-free on-off-keying (OOK) signals at a data rate of 25 Gbit/s with peak-to-peak drive voltages of only 180 mV_{pp}. This is the lowest drive voltage for error-free OOK signaling at 25 Gbit/s reported so far.

2. Device fabrication and characterization

The concept of the SOH Mach-Zehnder Modulator (MZM) is shown in Fig. 1a). The underlying silicon photonic base structure was fabricated on standard silicon-on-insulator (SOI) wafers in a commercial silicon (Si) foundry using 248 nm deep-UV (DUV) lithography process. Each arm comprises a slot waveguide consisting of two 240 nm-wide and 220 nm-high Si rails that are separated by a 160 nm-wide slot. The Si rails are electrically connected to an aluminum (Al) coplanar ground-signal-ground (GSG) transmission line by 70 nm-high doped Si slabs and Al vias. In a post-processing step, the slots are homogeneously filled by locally dispensing the organic EO material JRD1, whose chemical structure is depicted in Fig.1b). Both optical and RF field are highly confined in the slot, leading to a strong overlap which enables efficient EO modulation. Right after deposition, the EO material lacks a macroscopic EO effect since chromophores are randomly oriented, see Fig.1c). A macroscopic EO effect is only achieved upon electric-field poling. To this end, a DC poling voltage U_{pol} is applied across the floating ground electrodes, inducing an electric poling field (green arrows) inside the narrow slots. U_{pol} is applied at the elevated temperature such that the chromophores can align in an acentric orientation, which is maintained once the device has cooled down to room temperature, see Fig.1d). The device enables simple push-pull-operation: An RF signal applied to the MZM induces a field in the slots (red arrows) that is parallel to the orientation of the EO dipoles (green arrows) in the right and antiparallel in the other arm of the MZM. The schematic of the setup used for the static U_π characterization of the SOH MZM is depicted in Fig.1e). A low-frequency triangular waveform obtained from a function generator (FG) is applied to the signal electrode of the 1.5 mm-long MZM, while an optical CW signal at approximately 1550 nm is coupled to the device by an external-cavity laser (ECL). The modulated optical signal is detected by a low-speed photo diode (PD) and recorded by an oscilloscope, Fig.1f). The π-voltage can be directly read out and amounts to U_π = 213 mV, corresponding to a $U_\pi L$ of 320 Vµm. This is the lowest value ever reported for EO modulators based on low-loss dielectric waveguides. With the refractive index of JRD1, n_{EO} = 1.81, the

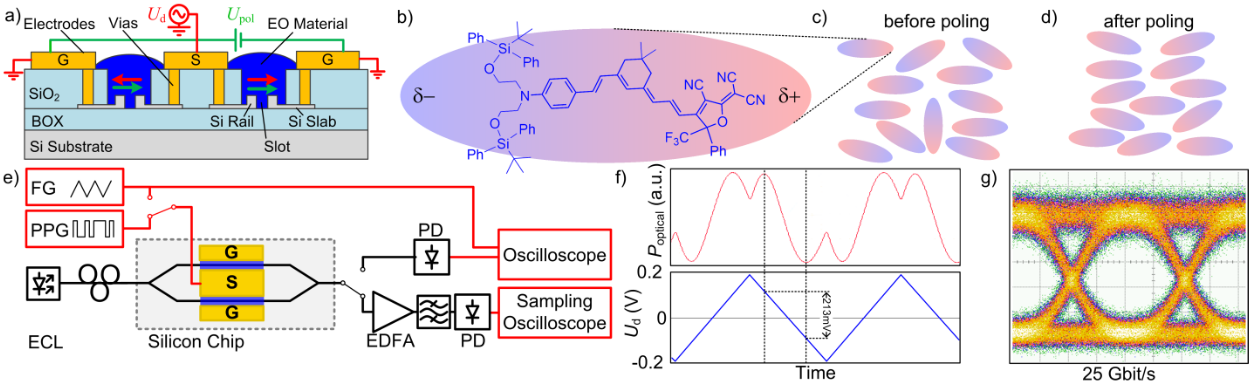

Fig.1. a) Cross section of the SOH MZM. Each arm consists of a silicon slot waveguide filled with the EO material JRD1. The Al GSG coplanar transmission line is connected via Al vias and conductive Si slabs to the Si rails. At elevated temperature, a poling voltage U_{pol} is applied across the floating ground electrodes, inducing an electric poling field (green arrows) within the slot. The dipoles of the EO material align along the poling field in acentric order. After cooling down, U_{pol} is removed and the acentric order of the chromophores is frozen in the EO material. A radio frequency (RF) signal voltage U_d induces electric fields in the slots (red arrows) that are antiparallel (parallel) to the aligned chromophores in the left (right) arm of the MZM, thereby realizing push-pull operation. b) Chemical structure of JRD1. c) Random orientation of JRD1 before poling. d) Acentric orientation of JRD1 after poling. e) Schematic of experimental setup for U_π and data transmission measurement. Signals obtained from a function generator (FG) or pulse pattern generators (PPG) are fed to the MZM via microwave probes. The optical carrier provided by an external-cavity laser (ECL) is coupled to and from the chip by grating couplers. A photo diode measures the slowly varying output light to determine U_π. The high-speed modulated light is amplified, filtered, and detected by a high speed PD connected to a sampling oscilloscope for recording eye diagrams. f) U_π measurement: Transmitted modulated optical power (red) and low frequency drive signal (blue) versus time, measured on the oscilloscope. Record-low $U_\pi = 213$ mV can be directly measured. g) Eye diagram for OOK signaling at 25 Gbit/s with a measured Q^2 factor of 17.3 dB and an estimated bit error ratio of 1.3×10^{-13} obtained for a drive voltage of 180 mV_{pp}.

measured value of $U_\pi L$ can be linked to an in-device EO coefficient of $r_{33} = 359$ pm/V [1]. To the best of our knowledge, this is the highest in-device material-related EO coefficient ever obtained for any material system.

4. Data transmission experiment

We further demonstrate the viability of the SOH MZM for high-speed data transmission. The experimental setup is shown in Fig.1e). A pseudo random bit sequence is obtained from a pulse pattern generator (PPG) and fed to the device by a microwave probe. The MZM is biased at its quadrature point and terminated by an external 50 Ω impedance. The fiber-to-fiber insertion loss amount to 18 dB and is caused by non-ideal grating couplers, lossy strip-to-slot converters, and Si slot waveguide losses. An erbium-doped fiber amplifier (EDFA) compensates for these losses, and a 0.6 nm band pass filter suppresses the amplified spontaneous emission noise of the EDFA before the optical signal is fed to a high-speed PD. The PD is connected to a sampling oscilloscope generating the eye diagram. Fig.1g) shows the eye diagram obtained for a drive voltage of 180 mV_{pp}, measured from the centers of gravity of the upper and lower rail of the electrical eye at a data rate of 25 Gbit/s. We measure a Q^2 factor of 17.3 dB and estimate a bit error ratio (BER) of 1.3×10^{-13}, which is well below the 10^{-9} threshold for error-free transmission.

5. Summary

We demonstrate an SOH MZM with record-high in-device nonlinearity of $r_{33} = 359$ pm/V. We show error-free transmission of an OOK signal at a data rate of 25 Gbit/s with record-low drive voltage of 180 mV_{pp}. These results pave the way towards ultra-efficient EO modulators that can be directly driven from sub-1V CMOS electronics [9].

This work was supported by the European Research Council (ERC Starting Grant 'EnTeraPIC', 280145), by the EU FP7 projects PhoxTroT and BigPipes, by the Alfried Krupp von Bohlen und Halbach Foundation, by the Helmholtz International Research School for Teratronics (HIRST), by the Karlsruhe School of Optics and Photonics (KSOP), and by the Karlsruhe Nano-Micro Facility (KNMF). The research of Larry Dalton was supported by the National Science Foundation (DMR-1303080) and the Air Force Office of Scientific Research (FA9550-15-1-0319).

6. References

[1] C. Koos *et al.*, "Silicon-Organic Hybrid (SOH) and Plasmonic-Organic Hybrid (POH) Integration," in J. Lightwave Technol., vol. 34, no. 2, pp. 256-268, Jan.15, 15 2016.
[2] S. Koeber ***et al.***, "Femtojoule electro-optic modulation using a silicon-organic hybrid device", Light Sci. Appl., vol. 4, no. 2, pp. e255, 2015.
[3] R. Palmer *et al.*, "High-Speed, Low Drive-Voltage Silicon-Organic Hybrid Modulator Based on a Binary-Chromophore Electro-Optic Material," in J. Lightwave Technol., vol. 32, no. 16, pp. 2726-2734, Aug.15, 15 2014.
[4] L. Alloatti, *et al.*, "42.7 Gbit/s electro-optic modulator in silicon technology," Opt. Express 19, 11841-11851 (2011)
[5] M. Lauermann *et al.*, "40 GBd 16QAM Signaling at 160 Gb/s in a Silicon-Organic Hybrid Modulator," in J. Lightwave Technol., vol. 33, no. 6, pp. 1210-1216, March15, 15 2015.
[6] W. Hartmann *et al.*, "100 Gbit/s OOK using a silicon-organic hybrid (SOH) modulator," 2015 European Conference on Optical Communication (ECOC), Valencia, 2015, pp. 1-3
[7] M. Lauermann, *et al.*, "Generation of 64 GBd 4ASK signals using a silicon-organic hybrid modulator at 80°C," Opt. Express 24, 9389-9396 (2016)
[8] W. W. Jin, *et al.*, "Benzocyclobutene barrier layer for suppressing conductance in nonlinear optical devices during electric field poling," Appl Phys Lett 104 (2014)
[9] S. Wolf, *et al.*, "DAC-Less Amplifier-Less Generation and Transmission of QAM Signals Using Sub-Volt Silicon-Organic Hybrid Modulators," in Journal of Lightwave Technology, vol. 33, no. 7, pp. 1425-1432, April1, 1 2015